

1 **Identification of Novel Syncytiotrophoblast Membrane Extracellular Vesicles Derived**
2 **Protein Biomarkers in Preeclampsia: A Cross-Sectional Study.**

3 Toluwalase AWOYEMI DPhil^{1*}, Shuhan JIANG MB;BS¹, Bríet BJARKADÓTTIR DPhil¹,
4 Ms. Maryam RAHBAR MSc¹, Prasanna LOGENTHIRAN MB;BS¹, Gavin COLLETT PhD,
5 Wei ZHANG PhD¹, Adam CRIBBS PhD², Ana Sofia CERDEIRA PhD¹ & Manu VATISH
6 DPhil¹

7

8

9 1 Nuffield Department of Women's & Reproductive Health, University of Oxford, Oxford,
10 United Kingdom

11 2 Nuffield Department of Orthopaedics, Rheumatology and Musculoskeletal Sciences,
12 University of Oxford, Oxford, United Kingdom

13

14

15

16

17

18

19

20 ***Corresponding author:** Dr Manu Vatish, MBBCh, BA (Hons), DPhil, MA, FMRCOG

21 Manu.vatish@wrh.ox.ac.uk, Phone number- +441865221009, Fax number-01865769141

22 **Address:** Nuffield Department of Women's and Reproductive Health, University of Oxford,
23 Women's Centre, John Radcliffe Hospital, Oxford OX3 9DU, United Kingdom

NOTE: This preprint reports new research that has not been certified by peer review and should not be used to guide clinical practice.

24 **Abstract**

25 **Background:** Preeclampsia (PE), a multi-systemic hypertensive pregnancy disease that affects
26 2-8% of pregnancies worldwide, is a leading cause of adverse maternal and fetal outcomes.
27 Current clinical PE tests have a low positive predictive value for PE prediction and diagnosis.
28 The placenta notably releases extracellular vesicles from the syncytiotrophoblast (STB-EV)
29 into the maternal circulation.

30 **Objective:** To identify a difference in placenta and STB-EV proteome between PE and normal
31 pregnancy (NP), which could lead to identifying potential biomarkers and mechanistic insights.

32 **Methods:** Using ex-vivo dual lobe perfusion, we performed mass spectrometry on placental
33 tissue, medium/large and small STB-EVs isolated from PE (n = 6) and NP (n = 6) placentae.
34 Bioinformatically, mass spectrometry was used to identify differentially carried proteins.
35 Western blot was used to validate the identified biomarkers. We finished our investigation with
36 an in-silico prediction of STB-EV mechanistic pathways.

37 **Results:** We identified a difference in the STB-EVs proteome between PE and NP. Filamin B,
38 collagen 17A1, pappalysin-A2, and scavenger Receptor Class B Type 1) were discovered and
39 verified to have different abundances in PE compared to NP. In silico mechanistic prediction
40 revealed novel mechanistic processes (such as abnormal protein metabolism) that may
41 contribute to the clinical and pathological manifestations of PE.

42 **Conclusions:** We identified potentially mechanistic pathways and identified differentially
43 carried proteins that may be important in the pathophysiology of PE and are worth investigating
44 because they could be used in future studies of disease mechanisms and as biomarkers.

45 **Funding:** This research was funded by the Medical Research Council (MRC Programme Grant
46 (MR/J0033601) and the Medical & Life Sciences translational fund (BRR00142 HE01.01)

47 **Keywords:** Syncytiotrophoblast membrane extracellular vesicles (STB-EVs), Preeclampsia,
48 Biomarkers, Proteomics, Placenta EVs, mechanisms

49 **Introduction**

50 Preeclampsia (PE) is a significant cause of maternal and neonatal morbidity and mortality,
51 affecting 2-8% of all pregnancies(Lisonkova & Joseph, 2013). It is characterized by
52 hypertension (systolic blood pressure ≥ 140 mmHg / diastolic pressure ≥ 90 mmHg), and either
53 proteinuria (protein/creatinine ratio of ≥ 30 mg/mmol or more), or evidence of maternal acute
54 kidney injury, liver dysfunction, neurological abnormalities, hemolysis, or thrombocytopenia,
55 and/or fetal growth restriction.(“ACOG Practice Bulletin No. 202: Gestational Hypertension
56 and Preeclampsia,” 2019; Brown et al., 2018) Predicting or early detection of PE is thus of
57 extreme importance to reduce the chance of long term complications but this has been
58 challenging due to the limitations of current predictive models and biochemical tests (which
59 lack in positive predictive value)(Zeisler et al., 2016). The existing tests perform far better in
60 ruling out rather than ruling in PE. They are also most effective shortly before the onset of the
61 disease and within a specific time frame (1 or 2 weeks) rather than earlier in
62 pregnancy(Thadhani et al., 2022).

63 The pathophysiology of PE implicates the placenta. It is known that PE can occur in
64 trophoblastic tumors (without the presence of a fetus); that PE is more common in multiple
65 pregnancy (with greater placental mass) and that it has occurred in ectopic pregnancies
66 (excluding the involvement of the uterus)(Billieux et al., 2004; Hailu et al., 2017; C. W. G.
67 Redman et al., 2022; Soto-Wright et al., 1995). Finally, delivery of the placenta (irrespective
68 of gestational age) is currently the only cure for the condition(C. Redman, 2014).

69 The placental syncytiotrophoblast (STB) layer, the interface between the fetus and the mother
70 which lies in direct contact with the maternal circulation. EVs, including STB-EVs, are
71 membrane-bound and cell-derived particles that carry different cargos, including proteins,
72 ribonucleic acid (RNA), deoxyribonucleic acid (DNA) and lipids(Raposo & Stoorvogel, 2013).
73 EVs are based on size into medium/large STB-EVs (MVs, 201–1000nm) or small STB-EVs

74 ($\leq 200\text{nm}$)(Dragovic et al., 2015b). The release of syncytiotrophoblast extracellular vesicles
75 (STB-EVs) into the maternal circulation increases with gestation and is further elevated in PE.
76 (Germain et al., 2007; Goswamia et al., 2006)
77 The presence of proteins, RNA species and DNA in EVs combined with their constitutional
78 release as inter-cellular signaling moieties means they also have potential in disease prediction
79 and diagnosis. In this study, we performed proteomic analysis of placenta and STB-EVs in PE
80 and NP to identify potential placenta-derived biomarkers. We also conducted in silico analysis
81 on the proteomes to detect potential molecular targets, mechanisms, and processes of PE.

82

83 **Methods**

84 **Ethics approval and patient information**

85 Oxfordshire Research Ethics Committee C (07/H0606/148) approved this study. Normal
86 pregnancy was a healthy singleton pregnancy with normal maternal blood pressure. PE was
87 defined as new (after 20 weeks) systolic blood pressure 140 mmHg or diastolic pressure 90
88 mmHg, proteinuria (protein/creatinine ratio of 30 mg/mmol or more), maternal acute kidney
89 injury, liver dysfunction, neurological features, haemolysis, thrombocytopenia, and/or foetal
90 growth restriction. This study included only early-onset PE patients (diagnosed before 34
91 weeks gestation). After informed consent, placenta was obtained from women undergoing
92 elective caesarian section without labor were collected.

93

94 **Placenta sample preparation and syncytiotrophoblast membrane extracellular vesicles** 95 **(STB-EVs) enrichment.**

96 Placenta biopsies were obtained adjacent to the perfused lobe and immediately frozen at -80°C
97 pending transfer to the Target Discovery Institute (Oxford) for proteomic analysis. We
98 obtained STB-EVs via placental perfusion as previously described(Dragovic et al., 2015a). Our

99 STB-EV enrichment and categorization process has been deposited on EV Track
100 (<http://www.EVTRACK.org>], EV-TRACK ID: EV 220157) with a score of 78% (the
101 average score on EV track for 2021 is 52 %). Full details can be found in the supplemental
102 data.

103

104 **Characterization of syncytiotrophoblast membrane extracellular vesicles (STB-EVs)**

105 Enriched STB-EVs were resuspended in filtered phosphate buffered saline (fPBS) and
106 characterized with bicinchoninic acid (BCA) assay (for protein concentration) and nanoparticle
107 tracking analysis (NTA) (for particle number and size profile). We also phenotyped the STB-
108 EVs with transmission electron microscopy (for morphology), flow cytometry (BD
109 Biosciences, LSRII), and western blot (for immunophenotyping). Flow cytometric analysis
110 was performed using antibodies to placental alkaline phosphatase – PLAP- (to confirm
111 syncytiotrophoblast origin), CD 41 (to identify co-isolated platelet EVs, CD235 a/b (to identify
112 co-isolated red blood cell EVs), HLA class I and II (to identify co-isolated white blood cell
113 EVs). Western blot was probed for placental alkaline phosphatase (PLAP [1.667 mg/ml] at
114 1:1000 dilution in house antibody), the known EV markers CD 63 ([200ug/ml] at 1:1000
115 dilution, Sc-59286, Santa Cruz Biotechnology), ALIX ([200ug/ml] at 1:1000 dilution, Sc-
116 53538, Santa Cruz Biotechnology) and the known negative EV marker Cytochrome C
117 ([200ug/ml] at 1:1000 dilution, Sc-13156, Santa Cruz Biotechnology) as recommended by the
118 international society for extracellular vesicles (ISEV) and subsequently incubated with the
119 corresponding secondary antibody anti-mouse, or anti-rabbit polyclonal goat
120 immunoglobulins/HRP (at 1: 2000 dilution, Dako UK Ltd, Cambridgeshire UK). Details of
121 nanoparticle tracking analysis and transmission electron microscopy can be found in the
122 supplemental data.

123

124 **Sample preparation for Mass Spectrometric analysis and bioinformatic analysis of**
125 **proteomic data from placenta tissue, medium/large, and small STB-EVs**

126 STB-EVs and placental tissue samples were processed for liquid chromatography mass
127 spectrometry (LC-MS) (Target Discovery Institute, Oxford). Raw label-free quantitation
128 (LFQ) data was imported and analyzed in Perseus (Max Planck Institute of Biochemistry).
129 Functional enrichment analysis was done with g: Profiler(Raudvere et al., 2019)
130 (<https://biit.cs.ut.ee/gprofiler/gost>) The mass spectrometry proteomics data have been
131 deposited to the ProteomeXchange Consortium via the PRIDE partner repository with the
132 dataset identifier PXD031953.

133

134 **Bioinformatic analysis of proteomic data from placenta tissue, medium/large and small**
135 **STB-EVs**

136 Perseus (Max Planck Institute of Biochemistry) was used for the analysis, along with the
137 accompanying documentation and tutorials. To remove invalid data, we pre-processed the raw
138 data by log transforming and filtering. Missing values were imputed at random from a normal
139 distribution using the following parameters: width = 0.3 and downshift = 1.8. To ensure
140 conformity to the normal distribution, the underlying distribution was visually inspected with
141 a histogram before and after missing data imputation. The data was then transformed further
142 by deducting each (transformed) value from the highest occurring protein expression value.

143 Principal component analysis (PCA), heatmaps, and Pearson correlation matrices were used to
144 further investigate the data. The data was analyzed using the correlation index and hierarchical
145 clustering. A two-sample independent student t-test was used to assess differential expression.
146 Multiple testing was corrected using permutation-based false discovery rate (FDR) with the
147 following parameters, with significance set at less than 0.05.

148 **Western Blotting**

149 To further characterize and immune-phenotype, we performed western blots on placental
150 homogenates and STB-EV pellets. The relevant primary antibodies were used to probe all STB-
151 EVs (as discussed in the main article). An equal amount of protein (20 micrograms) was mixed
152 with 4 X Laemmli buffer ((180 mM Tris-Cl (pH 6.8), 6% SDS, 30% glycerol, 0.3% 2-
153 mercaptoethanol, and 0.0015% bromophenol blue, BioRad)). After heating the sample mix for
154 ten minutes at 70°C, an equal volume of the sample mix was loaded. Electrophoresis was
155 performed at 150 V for 1.5 hours in a Novex minicell tank (Invitrogen, UK) filled with
156 NuPAGE™ MOPS SDS running buffer under reducing (for PLAP, Cytochrome C, ALIX, SR-
157 BI, Filamin B, PAPP-A2, Collagen 17 A1) and non-reducing (for CD 63) conditions on
158 NuPAGE™ 4-12% Bis-Tris Gel 1.0 mm x 10 well gels (Invitrogen by Thermo Fisher
159 Scientific) (Novex by Life Technologies). As a protein size marker, Precision plus protein™
160 dual color standards (Bio-Rad Laboratories Ltd, Hertfordshire, UK) were used. Following
161 protein separation, the proteins were transferred to a polyvinylidene difluoride (PVDF)
162 membrane (Bio-Rad).

163 In a Novex semi-dry transfer apparatus, the PVDF membrane and gel were sandwiched
164 between four filter paper sheets pre-soaked in anode one buffer solution (300 mM Tris, 10%
165 methanol pH 10.4) and two filter paper sheets pre-saturated with anode two buffer solution (25
166 mM Tris, 20% methanol pH 10.4) at the bottom and three filter paper sheets pre-soaked in
167 cathode buffer solution (25 mM Tris, 40 mM (Life Technologies, UK). For 45 minutes, the
168 transfer was run at 25 V. The membranes were blocked for one hour with 5% Blotto
169 (2BScientific) in 0.1% TBST (Tris-buffered saline (20 mM Tris, 137 mM NaCl, pH 7.6) and
170 1% Tween-20, Sigma), then incubated overnight with the appropriate antibody.

171 Antibodies used were SR-BI (ab52629 [0.35 $\mu\text{g}/\mu\text{l}$] 1:1000 dilution, monoclonal Rabbit,
172 Abcam), Filamin B (GTX387 [1.64 $\mu\text{g}/\mu\text{l}$] 1: 1000 dilution, monoclonal mouse, Insight
173 Biotechnology), PAPP-A2 (ab59100 [1 $\mu\text{g}/\mu\text{l}$] 1: 2000 dilution polyclonal Rabbit, Abcam),
174 Collagen 17 A1(ab28440 [1 $\mu\text{g}/\mu\text{l}$] 1: 2000 dilution polyclonal Rabbit, Abcam), and for
175 characterization, placental alkaline phosphatase (PLAP [1.667 $\mu\text{g}/\mu\text{l}$] at 1:1000 dilution in
176 house antibody), CD 63 ([200 $\mu\text{g}/\mu\text{l}$] at 1:1000 dilution, Sc-59286, Santa Cruz
177 Biotechnology), Alix ([200 $\mu\text{g}/\mu\text{l}$] at 1:1000 dilution, Sc-53538, Santa Cruz Biotechnology),
178 and Cytochrome C ([200 $\mu\text{g}/\mu\text{l}$] at 1:1000 dilution, Sc-13156, Santa Cruz Biotechnology) as
179 recommended by the international society for extracellular Vesicles (ISEV).

180 After an overnight incubation and three five-minute TBST washes, the membranes were
181 incubated for an hour at room temperature with the corresponding secondary antibody, anti-
182 mouse (P044701-2) or anti-rabbit (P044801-2) polyclonal goat immunoglobulins/ horseradish
183 peroxidase (HRP) (1: 2000 dilution, Dako UK Ltd, Cambridgeshire UK) and rinsed three times
184 in TBST. The membranes were developed using a gel documentation system (G-Box, Syngene,
185 Cambridge UK) running GeneSys (version 1.5.0.0, Syngene) and a chemiluminescence film
186 (Amersham HyperfilmTM ECL (enhanced chemiluminescence; GE Healthcare Limited,
187 Buckinghamshire UK) to obtain the band intensity for each lane. The fold change (FC) between
188 normal and preeclampsia samples was calculated by normalizing the comparative expression
189 analysis to the total protein loaded (using Amido Black stain) 17,18. The normalized
190 densitometric values were statistically tested using a one-tailed Student t-test, with significance
191 set at less than 0.05. Tables 1 and 2 show the reagents and antibodies used in western blot
192 analysis, respectively. Details of western blot for STB-EV characterization and proteomic
193 validation experiments can be seen in the supplemental material.

194

195 **Results**

196 *Patient demographics and clinical characteristics*

197 PE mothers (Table 1), as expected, had a significantly higher average systolic (178.83 mmHg,
198 $P < 0.001$) and diastolic (109.17 mmHg, $P < 0.001$) blood pressure compared to normal
199 pregnant mothers average systolic (129.50 mmHg) and diastolic (67.00 mmHg). PE women
200 are also significantly more likely to deliver prematurely (PE = 32.00 weeks gestation NP =
201 39.17 weeks gestation, $P < 0.001$) and have proteinuria (PE = 2.58 pluses on urine dipstick NP =
202 = 0 pluses on urine dipstick, $P < 0.001$) compared to normal pregnancy
203 Finally, PE babies significantly weighed less than normal babies (PE = 1515.83g NP = 3912.50
204 g, $P < 0.001$). Surprisingly, we found no significant difference in body mass index, the gender
205 of the child, and maternal age.

206

207

208

209

210

211

212

213

214

215

216

217

218

219

220 **Table 1.** General descriptive statistics of sample population

Characteristics	Sub-Classification	Normal		P
		Pregnancy	Preeclampsia	Value
Sample size		6	6	
Maternal age years (mean (SD))		34.50 (5.39)	36.33(4.13)	0.524
Systolic blood pressure mmHg (mean (SD))		129.50 (4.93)	178.83(12.56)	<0.001
Diastolic blood pressure mmHg (mean (SD))		67.00 (6.20)	109.17(9.85)	<0.001
Body mass index kg/m-2 (mean (SD))		29.92(9.10)	31.25(11.12)	0.825
Proteinuria plus(es) (mean (SD))		0	2.58(1.20)	<0.001
Gestational age at delivery in weeks (mean (SD))		39.17 (0.98)	32.00(3.52)	0.001
Birth weight grams (mean (SD))		3912.50 (730.40)	1515.83(600.57)	<0.001
Intrauterine growth restriction (IUGR) =				
Yes (%)		0(0)	6(100)	0.004
Male new-born gender (%)		2(33.3)	2(33.3)	1.000

221

222 **Characterization of syncytiotrophoblast membrane extracellular vesicles (STB-EVs)**

223 Flow cytometry (Figure 1) was showed that many detected events ($83-85 \pm 8.0-8.3\%$) were
 224 negative for CD 235a (Red blood cells), CD41 (platelets) and HLA-I and II (white blood cells)
 225 (Figure 1B) while $92 \pm 0.9\%$ (Figure 1D and 1G) of detected events were PLAP⁺ extracellular
 226 vesicles (BODIPY FL N-(2-aminoethyl)-maleimide (bioM) and placental alkaline phosphatase
 227 (PLAP) double-positive). Detergent treatment with NP-40 confirmed that majority (99%) of

228 our samples were vesicular our samples were largely vesicular since only $0.1 \pm 0.12\%$ of
229 BODIPY FL N-(2-aminoethyl)-maleimide and PLAP double-positive events were detected (a
230 reduction of 99%) (Figure 1E and 1H).

231 Transmission electron microscopy on 10K STB-EV pellets (Figure 2B and 2C) and 150K STB-
232 EVs (Figure 2E and 2F) in our sample preparation showed the typical cup-shaped morphology
233 of extracellular vesicles on transmission electron microscopy (TEM) within the appropriate
234 size range. Western blot confirmed they express the classic syncytiotrophoblast membrane
235 marker, placenta alkaline phosphatase (PLAP), the extracellular vesicle markers ALIX and CD
236 63. In addition, they lacked the negative EV marker cytochrome C (Figure 2G). Nanoparticle
237 tracking analysis (NTA) confirmed the homogeneity of the 150K STB-EV pellets (small STB-
238 EVs) (Figure 2A) with a modal size of (205.8 ± 67.7) nm and the heterogeneity of the 10K
239 STB-EV pellets (medium/large STB-EVs) (Figure 2D) with a size range of (479.4 ± 145.6)
240 nm.

241

242

243

244

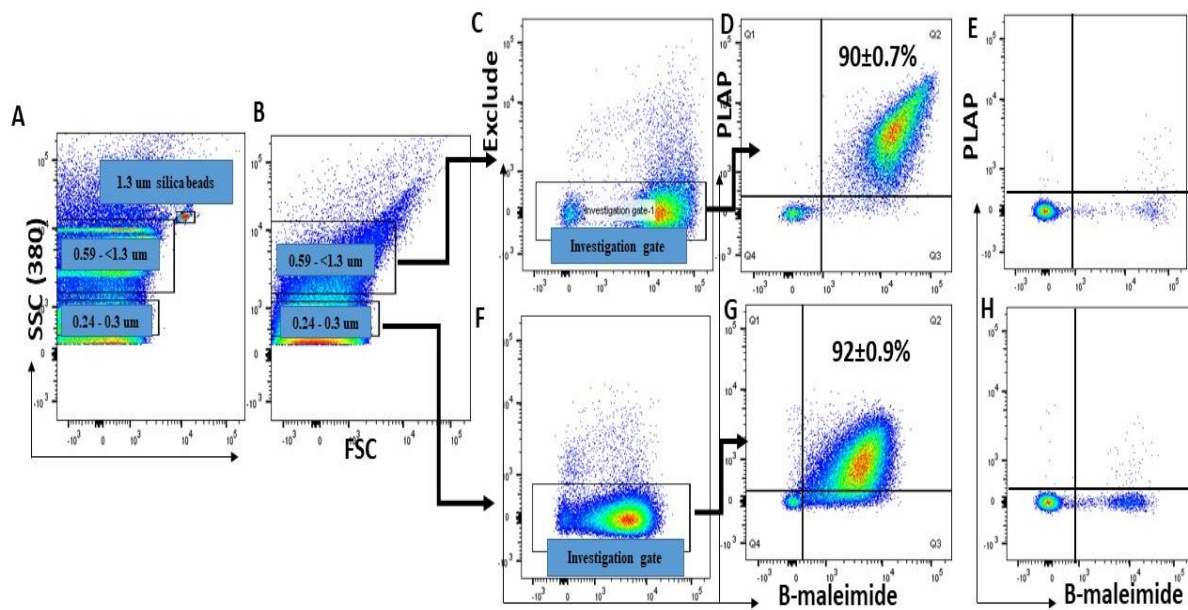
245

246

247

248

249



250

251

252 **Figure 1.** Flow analysis of medium/large STB-EVs in the 10K STB-EV pellet. Apogee beads

253 mix were used to set the flow machine's light scatter resolution to 0.59-1.3 mm and 0.24-1.3

254 (A) mm silica beads. Figures B show the application of SSC and FSC PMTVs as determined

255 by apogee beads mix for the analysis of m/ISTB-EVs in the 10K pellet. An investigation gate

256 was created to include only medium/large EVs negative for non-placental markers (C & F).

257 Extracellular vesicles from the investigation gate were further analyzed for staining by bioM

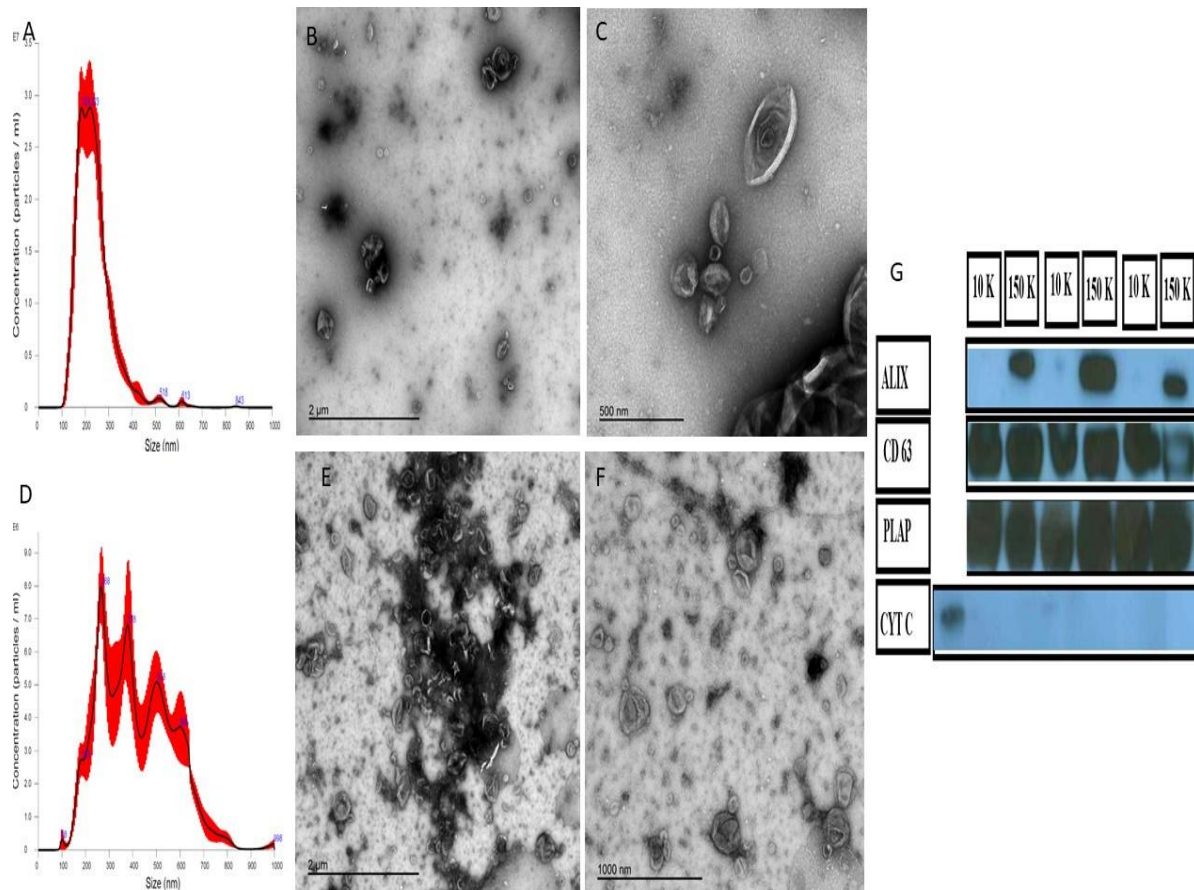
258 and expression of PLAP (D & G). Figure E and H shows that the bioM⁺ PLAP⁺ EVs were

259 sensitive to detergent treatment. The percent of B-Maleimide⁺ PLAP⁺ from the 0.59-1.3 micron

260 gate is consistent under both SSC conditions.

261

262



263

264

265 **Figure 2.** Results of STB-EV characterization. Figure 2A and 2D show the NTA results of S
266 STB-EVs (2D) and m/STB-EVs (2A). Figure 2B,2C,2E and 2F displays representative
267 transmission electron microscopy (TEM) images with wide view (2B and 2E), medium/large
268 STB-EVs (2C), and Small STB-EVs (2F).

269

270

271

272

273

274

275

276 *Differentially carried proteins (DCPs) in Placenta homogenate, Medium/Large STB-EVs*
277 *and Small STB-EVs in Preeclampsia versus normal pregnancies.*

278 In total, using mass spectrometry, there fifteen (15) proteins in the placenta, three hundred and
279 four (304) in m/ISTB-EVs, and seventy-three (73) in sSTB-EVs were differentially expressed
280 between preeclampsia (PE) and normal pregnancy (NP).

281 In the placenta (Table 2), *isoform HMG-R of High mobility group protein (HMGAI)*,
282 *Fibrinogen-like protein 1(FGL1)*, *isoform 1 of Kinesin-like protein (KIF2A)*, *Ig kappa chain C*
283 *region (IGKC)* were the most abundant proteins based on fold change. Concomitantly, *serum*
284 *paraoxonase/arylesterase 1 (PON1)* and *alpha-1B-glycoprotein (AIBG)* were the least
285 abundant proteins.

286 For m/ISTB-EVs (Table 2), the most differentially abundant proteins were the *collagen alpha-*
287 *1(XVII) chain (COL17A1)*, *isoform 2 of Filamin-B (FLNB)*, *tumor necrosis factor-alpha-*
288 *induced protein 2 (Fragment) (TNFAIP2)* based on fold change. In contrast, the least
289 differentially abundant proteins were *sodium-dependent phosphate transporter 1 (SLC20A1)*,
290 *methylthioribose-1-phosphate isomerase (Fragment) (MRI1)*, *prostatic acid phosphatase*
291 *(Fragment) (ACPP)* based on fold change.

292 Finally, the sSTB-EVs (Table 2) had *solute carrier family 2, facilitated glucose transporter*
293 *member (SLC2A11)*, *v-type proton ATPase 16 KDa proteolipid subunit (ATP6V0C)*,
294 *pappalysin 2 (PAPP-A2)* as the most differentially abundant by fold change while *sodium-*
295 *dependent phosphate transporter 1 (SLC20A1)* and *isoform 2 of ADP-ribosylation factor*
296 *GTPase-activating protein (ARFGAP3)* were the least differentially abundant. There were 25
297 differentially carried proteins (DCPs) including *filamin B (FLNB)*, *ERO1-like protein alpha*
298 *(ERO1A)*, *endoglin (EGLN)*, *pappalysin-2 (PAPP-A2)*, *siglec6 (SIGL6)* shared between
299 m/ISTB-EVS and sSTB-EVs and only one protein, *isoform 1 of kinesin-like protein (KIF2A)*

300 shared between the placenta and the m/l STB-EVs. Only one protein *chloride intracellular*
301 *channel protein 3 (CLIC3)*, was found in all three sample sub-types (Table 3).

302

303

304

305

306

307

308

309

310

311

312

313

314

315

316

317

318

319

320

321

322

323

324 **Table 2:** Top ten differentially expressed Proteins between normal and preeclampsia placentas
 325 (bold font), medium/large STB-EVs (normal font), small STB-EVs(italics)

Protein	Symbol	LFC	Adjusted P. Value
Placenta			
Isoform HMG-R of High mobility group protein HMG-I/HMG-Y	HMGA1	3.14	0.03
Fibrinogen-like protein 1	FGL1	2.49	0.04
Isoform 1 of Kinesin-like protein KIF2A	KIF2A	1.47	0.02
Chloride intracellular channel protein 3	CLIC3	1.09	0.05
Mesencephalic astrocyte-derived neurotrophic factor	MANF	1.02	0.03
Ig kappa chain V-I region AG	KV101	-1.02	0.05
Haloacid dehalogenase-like hydrolase domain-containing protein 2 (Fragment)	K7EJQ8	-1.23	0.05
Ig kappa chain C region	IGKC	-1.27	0.05
Alpha-1B-glycoprotein	A1BG	-1.34	0.05
Serum paraoxonase/arylesterase 1	PON1	-2.18	<0.01
Medium/Large STB-EVs			
Collagen alpha-1(XVII) chain	COL17A1	4.79	<0.01
Isoform 2 of Filamin B	FLNB	3.09	<0.01
Tumor necrosis factor alpha-inducible protein	TNFAIP2	3.03	<0.01
Minor histocompatibility antigen	HMHA1	1.59	0.03
Bridging integrator 2	BIN2	2.33	0.02

Sodium/potassium-transporting ATPase subunit			
beta-1	ATP1B	1.99	0.02
ERO-1 like protein alpha	ERO1L	1.97	<0.01
Endoglin	ENG	1.82	<0.01
Methylthioribose-1-phosphate isomerase			
(Fragment)	MRI1	-1.96	0.04
Sodium-dependent phosphate transporter 1	S20A1/SLC17A1	-5.24	0.04
Small STB-EVs			
<i>Solute carrier family 2, facilitated glucose transporter member 11</i>			
	<i>SLC2A11</i>	<i>8.91</i>	<i>0.01</i>
<i>V-type proton ATPase 16 kDa proteolipid subunit</i>			
	<i>VATL</i>	<i>7.25</i>	<i>0.02</i>
<i>Pappalysin-2</i>	<i>PAPP2</i>	<i>3.76</i>	<i>0.02</i>
<i>ERO1-like protein alpha</i>	<i>ERO1A</i>	<i>3.29</i>	<i>0.02</i>
<i>Isoform 2 of Creatine kinase U-type, mitochondrial</i>			
	<i>KCRU</i>	<i>3.20</i>	<i>0.02</i>
<i>SCARB1 protein</i>	<i>B7ZKQ9</i>	<i>2.95</i>	<i>0.05</i>
<i>Isoform 2 of Filamin-B</i>	<i>FLNB</i>	<i>2.92</i>	<i>0.02</i>
<i>Solute carrier organic anion transporter family member 2A1</i>			
	<i>SO2A1</i>	<i>2.86</i>	<i>0.02</i>
<i>Isoform 2 of Oligaccharyltransferase complex subunit TC</i>			
	<i>OSTC</i>	<i>2.82</i>	<i>0.02</i>
<i>SCY1-like protein 2</i>	<i>SCYL2</i>	<i>2.71</i>	<i>0.02</i>
<i>Sodium-dependent phosphate transporter 1</i>	<i>S20A1</i>	<i>-2.93</i>	<i>0.01</i>

327

328

329

330

331

332

333

334

335

336

337

338

339

340

341

342

343

344

345

346

347

348

349

350

351 **Table 3.** List of overlapping differentially carried proteins in the placenta, medium/large STB-
 352 EVs and small STB-EVs

Sample types	Differentially expressed proteins (DEPs)
m/ISTB-EVs and Placenta	Kinesin-like protein
m/ISTB-EVs, sSTB-EVs and Placenta	Chloride intracellular channel protein 3
m/ISTB-EVs and sSTB-EVs	Filamin B
	Endoplasmic Reticulum Oxidoreductase Alpha
	X-linked retinitis pigmentosa GTPase regulator interacting protein 1
	Protein NDRG1
	Collagen alpha 1(XVII) chain
	Monocyte differentiation antigen CD14
	Trophoblast glycoprotein
	Heat shock-related 70 kDa protein 2
	Endoglin
	Hippocalcin-like protein 1
	SCARB1 protein
	Importin subunit alpha 7
	Protein BCAP
	Endothelial protein C receptor
	Caveolin
	Pappalysin-2

Phosphatidylinositol 3-kinase regulatory subunit alpha
Keratin, type I cytoskeletal 19
Siglec6
Protein disulfide-isomerase
Amine oxidase [flavin-containing] A
Copine-3
Dolichyl-diphosphooligosaccharide
Sodium-dependent phosphate transporter 1
Annexin A4

353

354

355

356

357

358

359

360

361

362

363

364

365

366

367

368 **Validation of select proteins in the placenta homogenate, medium/Large STB-EVs, and**
369 **small STB-EVs**

370 We combined all the DCPs identified from the placenta, m/lSTB-EVs, and sSTB-EVs and
371 selected proteins to validate based on fold change and our placenta specificity or enrichment
372 as previously described above in the methods section. These were pappalysin A2 (*PAPP-A2*),
373 *collagen 17A1 (COL17A1)*, *filamin B*, and *scavenger receptor class B type I (SR-BI/ SCARB1)*.
374 Validation was performed by western blot on all sample sub-types.

375 In the placenta (Figure 3A and 3D), *PAPP-A2* (FC =6.39, P Value = 0.0001) and *SR-BI* (FC =
376 1.72, P Value = 0.04) were all differentially abundant in PE. *Filamin B* (FC = 2.59, P Value =
377 0.12) was differentially abundant in PE but not significant while *COL17A1* was undetectable.
378 In medium/large STB-EVs (Figure 3B and 3E), pappalysin A2 (FC =5.09, P Value = 0.004),
379 *collagen 17A1* (FC =71.21, P Value = 0.002), *filamin B* (FC =7.60, P Value = 0.014) and
380 *scavenger receptor class B type I* (FC =2.28, P Value = 0.018) were all significantly
381 differentially abundant in PE compared to normal. In sSTB-EVs (Figure 3C and 3F), only
382 *filamin B* (FC =7.73, P Value = 0.003) and *SR-BI/SCARB1* (FC =1.60, P Value = 0.002) were
383 significantly differentially abundant while *COL17A1*(FC =12.79, P Value = 0.07) and *PAPP-*
384 *A2* (FC =1.48, P Value = 0.11) were differentially abundant but not significantly so.

385

386 **Functional enrichment of differentially carried proteins (DCPs) in preeclampsia (PE)**

387 We performed a functional enrichment analysis on the list of differentially carried proteins in
388 placenta tissue, medium/large STB-EVs, and small STB-EVs to help better understand their
389 role in preeclampsia (PE). The three sample sub-types did not have overlapping gene ontology
390 terms or KEGG pathways. The top biological processes overrepresented in the placenta (Table
391 3A) were processes that involve *neurotransmitter secretion and transport*. In comparison, the
392 enriched biological processes in the m/lSTB-EVs (supplemental table 3) *involved responses to*

393 *hypoxia*. Finally, *posttranslational protein modification processes* were enriched among small
394 STB-EVs (supplemental table 3). *Neurotrophin signaling pathway*, *spinocerebellar ataxia*,
395 *and protein processing pathway* were among the over enriched KEGG pathways in the
396 placenta, m/ISTB-EVs and sSTB-EVs respectively (Supplemental table 4).

397

398 **Discussion**

399 **Principal findings**

400 In our analysis, PE and NP have different placenta and STB-EV proteomes. Four STB-EV
401 biomarkers—filamin B, collagen 17A1, pappalysin-A2, and scavenger Receptor Class B Type
402 1—were verified for differential abundance. In silico investigation revealed molecular
403 pathways such abnormal protein metabolism that may contribute to PE's clinical and
404 pathological symptoms and inform future research.

405 **Results in the context of what is known.**

406 Our analysis found chloride intracellular channel 3 (CLIC3) to be the only protein differentially
407 abundant among all sample types. CLIC3 is expressed in the placenta throughout
408 pregnancy(Money et al., 2007) and is abundant in PE placentas compared to NP, a finding
409 corroborated by our results. However, it has not previously been described in terms of STB-
410 EVs. CLIC3 also recycles activated integrins back to the plasma membrane and facilitates cell
411 migration and invasion(Dozynkiewicz et al., 2012) a process that has been identified as
412 abnormal in PE(KHONG et al., 1986).

413 We found *COL17A1* to be more abundant in PE m/ISTB-EVs but not detectable in the placenta
414 in both normal and PE. Although collagen 17 has not been described in preeclampsia, a protein
415 of the same family, collagen 1 is deposited in higher amounts in the PE placenta and can induce
416 preeclampsia-like symptoms by suppressing the proliferation and invasion of trophoblasts.
417 This suppression was reversible by treating with ERK and B-catenin agonists(Feng et al.,

418 2021). Likewise, *PAPP-A2* was significantly more abundant in the PE placenta and m/ISTB-
419 EVs. *PAPP-A2* cleaves insulin-like growth factor binding protein (IGFBP-5 and, to a lesser
420 extent, IGFBP-3). *PAPP-A2*'s mRNA and protein are differentially expressed in the placenta
421 and maternal serum in PE patients(Whitehead et al., 2013).

422 Filamin B was significantly more abundant in PE m/ISTB-EVs and sSTB-EVs compared to
423 NP. Filamin B participates in cellular structural mechanics and signal transduction by
424 interacting with ion channels, signaling molecules, transmembrane proteins, and transcription
425 factors(Zhou et al., 2010). It also suppresses tumor growth and metastasis(Iguchi et al., 2015).
426 Interestingly, in contrast to our study wei et al described Filamin B as being up regulated in the
427 placenta (Wei et al., 2019) . Wei et al used glyceraldehyde 3-phosphate dehydrogenase
428 (GAPDH) as an internal reference while we used total protein normalization to Amido black
429 to quantify and compare protein expression. GAPDH is an unreliable internal reference protein,
430 particularly in preeclampsia(Lanoix et al., 2012) and this may explain these discordant
431 findings. In addition, in our proteomics data, we found GAPDH to be among the most
432 differentially expressed proteins.

433 Likewise, we identified scavenger receptor class B, type 1 (SCARB1/SR-BI) to be significantly
434 increased in PE placenta, m/l and sSTB-EVs. SCARB1/SR-BI, is most abundant in the adrenal
435 glands, placenta, liver, and brain(Ganesan et al., 2016; Shen et al., 2016). SR-BI facilitates the
436 uptake of cholesteryl esters from high-density lipoproteins and lipid-soluble vitamin and
437 transthyretin-bound thyroid hormone by placental trophoblast cells(Landers et al., 2018).

438 In terms of potential mechanisms of preeclampsia, we found no overlap in the biological
439 processes and KEGG pathways among the three sample sub-type. In the placenta, gene
440 ontology biological processes (GO: BP) involved in *neurotransmitter secretion and transport*
441 were overrepresented while *platelet activation*, *MAPK* and *Rap 1 signaling* pathways were
442 among the detected KEGG pathways. In m/ISTB-EVs, *protein modification process*, and

443 *decreased oxygen level responses* were among the perturbed GO: BP terms. *Alzheimer's* and
444 *prion disease* were among the identified KEGG pathways. In sSTB-EVs, *post-translational*
445 *modification processes* and *endoplasmic reticulum protein processing* were the principal GO:
446 BP terms and KEGG pathways.

447 Recent research has shown that ischemic hypoxia and the release of proinflammatory cytokines
448 in PE can cause protein misfolding and initiate endoplasmic reticulum (ER) stress due to
449 hypoxia-reoxygenation damage to the endoplasmic reticulum(Gathiram & Moodley, 2016). PE
450 can also cause posttranslational modifications to proteins, such as changing the isoelectric
451 point, which results in different S-nitrosylation outcomes in placental proteins(Zhang et al.,
452 2011). It is thought that the accumulation of these aggregates of unfolded protein response
453 (UPR) or misfolded proteins contributes to the pathophysiology of PE(Gathiram & Moodley,
454 2016). Other processes and KEGG pathways have been previously described in preeclampsia,
455 while others found in our study are new and may warrant further research(Lee et al., 2020;
456 Wan Shumei, Peng Ping, Qiao Lin, 2019).

457 **Ideas and Speculation**

458 STB-EVs are liquid biomarkers with real-time information from the damaged placenta in PE
459 due to their placenta-specificity. It would be interesting to test maternal plasma or serum
460 samples for the four STB-EV indicators reported in our study.

461 It is unclear which comes first: misfolded proteins depositing in trophoblasts and preventing
462 normal invasion, causing ischemia and endoplasmic reticulum stress, which leads to defects in
463 trophoblast invasion, oxidative stress, and endothelial cell dysfunction, or the trophoblast
464 invasion defects, oxidative stress, and endothelial cell dysfunction, or the misfolded proteins
465 because of faulty invasion and oxidative stress. Further studies exploring these PE pathogenic
466 processes would be intriguing.

467

468 **Strengths and limitations**

469 Our study explored the difference in the proteome between PE and NP by analyzing the
470 placenta and its extracellular vesicles. This study is one of the few to do so using extracellular
471 vesicles obtained by a physiologic technique, the *ex-vivo* dual lobe placenta perfusion.
472 However, the control population used for this study was not gestationally age-matched because
473 it is impossible to obtain the ideal control for early onset PE patients. Also, our sample size
474 was small (n of 12).

475 **Conclusion**

476 Our study may have found novel STB-EV-bound protein indicators that are significantly more
477 abundant in PE than normal. Since STB-EVs are present in the circulation from early
478 pregnancy to term and are released more in PE, these STB-EV carried proteins may help with
479 earlier diagnosis and mechanistic insights.

480 **Acknowledgments**

481 We acknowledge the support of the National Institute of Health Research Clinical Research
482 Network for assistance in patient recruitment and Fenella Roseman and Lotoyah Carty,
483 research midwives who kindly recruited the patients for this study. We acknowledge the
484 patients who kindly consented to this research study.

485 **Competing interests:**

486 The authors declare no competing interests.

487

488

489

490

491 References

- 492 ACOG Practice Bulletin No. 202: Gestational Hypertension and Preeclampsia. (2019).
493 *Obstetrics and Gynecology*. <https://doi.org/10.1097/AOG.0000000000003018>
- 494 Billieux, M. H., Petignat, P., Fior, A., Mhawech, P., Blouin, J. L., Dahoun, S., & Vassilakos,
495 P. (2004). Pre-eclampsia and peripartum cardiomyopathy in molar pregnancy: clinical
496 implication for maternally imprinted genes. *Ultrasound in Obstetrics & Gynecology : The*
497 *Official Journal of the International Society of Ultrasound in Obstetrics and Gynecology*,
498 23(4), 398–401. <https://doi.org/10.1002/UOG.1015>
- 499 Brown, M. A., Magee, L. A., Kenny, L. C., Karumanchi, S. A., McCarthy, F. P., Saito, S., Hall,
500 D. R., Warren, C. E., Adoyi, G., & Ishaku, S. (2018). Hypertensive disorders of
501 pregnancy: ISSHP classification, diagnosis, and management recommendations for
502 international practice. In *Hypertension*.
503 <https://doi.org/10.1161/HYPERTENSIONAHA.117.10803>
- 504 Dozynkiewicz, M. A., Jamieson, N. B., MacPherson, I., Grindlay, J., vandenBerghe, P. V. E.,
505 vonThun, A., Morton, J. P., Gourley, C., Timpson, P., Nixon, C., McKay, C. J., Carter,
506 R., Strachan, D., Anderson, K., Sansom, O. J., Caswell, P. T., & Norman, J. C. (2012).
507 Rab25 and CLIC3 Collaborate to Promote Integrin Recycling from Late
508 Endosomes/Lysosomes and Drive Cancer Progression. *Developmental Cell*, 22(1), 131.
509 <https://doi.org/10.1016/J.DEVCEL.2011.11.008>
- 510 Dragovic, R. A., Collett, G. P., Hole, P., Ferguson, D. J. P., Redman, C. W., Sargent, I. L., &
511 Tannetta, D. S. (2015a). Isolation of syncytiotrophoblast microvesicles and exosomes and
512 their characterisation by multicolour flow cytometry and fluorescence Nanoparticle
513 Tracking Analysis. *Methods*, 87, 64–74. <https://doi.org/10.1016/j.ymeth.2015.03.028>
- 514 Dragovic, R. A., Collett, G. P., Hole, P., Ferguson, D. J. P., Redman, C. W., Sargent, I. L., &
515 Tannetta, D. S. (2015b). Isolation of syncytiotrophoblast microvesicles and exosomes and
516 their characterisation by multicolour flow cytometry and fluorescence Nanoparticle
517 Tracking Analysis. *Methods (San Diego, Calif.)*, 87, 64–74.
518 <https://doi.org/10.1016/J.YMETH.2015.03.028>
- 519 Feng, Y., Chen, X., Wang, H., Chen, X., Lan, Z., Li, P., Cao, Y., Liu, M., Lv, J., Chen, Y.,
520 Wang, Y., Sheng, C., Huang, Y., Zhong, M., Wang, Z., Yue, X., & Huang, L. (2021).
521 Collagen I Induces Preeclampsia-Like Symptoms by Suppressing Proliferation and
522 Invasion of Trophoblasts. *Frontiers in Endocrinology*, 12.
523 <https://doi.org/10.3389/fendo.2021.664766>
- 524 Ganesan, L. P., Mates, J. M., Cheplowitz, A. M., Avila, C. L., Zimmerer, J. M., Yao, Z.,
525 Maiseyeu, A., Rajaram, M. V. S., Robinson, J. M., & Anderson, C. L. (2016). Scavenger
526 receptor B1, the HDL receptor, is expressed abundantly in liver sinusoidal endothelial
527 cells. *Scientific Reports*, 6. <https://doi.org/10.1038/srep20646>
- 528 Gathiram, P., & Moodley, J. (2016). Pre-eclampsia: its pathogenesis and pathophysiology.
529 *Cardiovascular Journal of Africa*, 27(2), 71–78. <https://doi.org/10.5830/CVJA-2016-009>
- 530 Germain, S. J., Sacks, G. P., Sooranna, S. R., Soorana, S. R., Sargent, I. L., & Redman, C. W.
531 (2007). Systemic inflammatory priming in normal pregnancy and preeclampsia: the role
532 of circulating syncytiotrophoblast microparticles. *Journal of Immunology (Baltimore,*
533 *Md. : 1950)*, 178(9), 5949–5956. <https://doi.org/10.4049/JIMMUNOL.178.9.5949>
- 534 Goswamia, D., Tannetta, D. S., Magee, L. A., Fuchisawa, A., Redman, C. W. G., Sargent, I.
535 L., & von Dadelszen, P. (2006). Excess syncytiotrophoblast microparticle shedding is a
536 feature of early-onset pre-eclampsia, but not normotensive intrauterine growth restriction.
537 *Placenta*, 27(1), 56–61. <https://doi.org/10.1016/J.PLACENTA.2004.11.007>

- 538 Hailu, F. G., Yihunie, G. T., Essa, A. A., & Tsega, W. kindie. (2017). Advanced abdominal
539 pregnancy, with live fetus and severe preeclampsia, case report. *BMC Pregnancy and*
540 *Childbirth*, 17(1). <https://doi.org/10.1186/S12884-017-1437-Y>
- 541 Iguchi, Y., Ishihara, S., Uchida, Y., Tajima, K., Mizutani, T., Kawabata, K., & Haga, H. (2015).
542 Filamin B enhances the invasiveness of cancer cells into 3D collagen matrices. *Cell*
543 *Structure and Function*, 40(2). <https://doi.org/10.1247/csf.15001>
- 544 KHONG, T. Y., de WOLF, F., ROBERTSON, W. B., & BROSENS, I. (1986). Inadequate
545 maternal vascular response to placentation in pregnancies complicated by pre-eclampsia
546 and by small-for-gestational age infants. *BJOG: An International Journal of Obstetrics &*
547 *Gynaecology*, 93(10). <https://doi.org/10.1111/j.1471-0528.1986.tb07830.x>
- 548 Landers, K. A., Li, H., Mortimer, R. H., McLeod, D. S. A., d'Emden, M. C., & Richard, K.
549 (2018). Transthyretin uptake in placental cells is regulated by the high-density lipoprotein
550 receptor, scavenger receptor class B member 1. *Molecular and Cellular Endocrinology*,
551 474. <https://doi.org/10.1016/j.mce.2018.02.014>
- 552 Lanoix, D., St-Pierre, J., Lacasse, A. A., Viau, M., Lafond, J., & Vaillancourt, C. (2012).
553 Stability of reference proteins in human placenta: General protein stains are the
554 benchmark. *Placenta*, 33(3). <https://doi.org/10.1016/j.placenta.2011.12.008>
- 555 Lee, A., Chow, L., Skeith, L., Nicholas, J. A., Poon, M.-C., Poole, A. W., & Agbani, E. O.
556 (2020). Platelet Membrane Procoagulation in Preeclampsia. *Blood*, 136(Supplement 1).
557 <https://doi.org/10.1182/blood-2020-137213>
- 558 Lisonkova, S., & Joseph, K. S. (2013). Incidence of preeclampsia: risk factors and outcomes
559 associated with early- versus late-onset disease. *American Journal of Obstetrics and*
560 *Gynecology*, 209(6), 544.e1-544.e12. <https://doi.org/10.1016/J.AJOG.2013.08.019>
- 561 Money, T. T., King, R. G., Wong, M. H., Stevenson, J. L., Kalionis, B., Erwich, J. J. H. M.,
562 Huisman, M. A., Timmer, A., Hiden, U., Desoye, G., & Gude, N. M. (2007). Expression
563 and Cellular Localisation of Chloride Intracellular Channel 3 in Human Placenta and Fetal
564 Membranes. *Placenta*, 28(5-6), 429-436.
565 <https://doi.org/10.1016/J.PLACENTA.2006.08.002>
- 566 Raposo, G., & Stoorvogel, W. (2013). Extracellular vesicles: Exosomes, microvesicles, and
567 friends. *Journal of Cell Biology*, 200(4), 373-383.
568 <https://doi.org/10.1083/JCB.201211138>
- 569 Raudvere, U., Kolberg, L., Kuzmin, I., Arak, T., Adler, P., Peterson, H., & Vilo, J. (2019).
570 G:Profiler: A web server for functional enrichment analysis and conversions of gene lists
571 (2019 update). *Nucleic Acids Research*, 47(W1). <https://doi.org/10.1093/nar/gkz369>
- 572 Redman, C. (2014). Pre-eclampsia: A complex and variable disease. *Pregnancy Hypertension*,
573 4(3), 241-242. <https://doi.org/10.1016/J.PREGHY.2014.04.009>
- 574 Redman, C. W. G., Staff, A. C., & Roberts, J. M. (2022). Syncytiotrophoblast stress in
575 preeclampsia: the convergence point for multiple pathways. *American Journal of*
576 *Obstetrics and Gynecology*, 226(2S), S907-S927.
577 <https://doi.org/10.1016/J.AJOG.2020.09.047>
- 578 Shen, W. J., Azhar, S., & Kraemer, F. B. (2016). ACTH regulation of adrenal SR-B1. In
579 *Frontiers in Endocrinology* (Vol. 7, Issue MAY).
580 <https://doi.org/10.3389/fendo.2016.00042>
- 581 Soto-Wright, V., Bernstein, M., Goldstein, D. P., & Berkowitz, R. S. (1995). The changing
582 clinical presentation of complete molar pregnancy. *Obstetrics and Gynecology*, 86(5),
583 775-779. [https://doi.org/10.1016/0029-7844\(95\)00268-V](https://doi.org/10.1016/0029-7844(95)00268-V)
- 584 Thadhani, R., Lemoine, E., Rana, S., Costantine, M. M., Calsavara, V. F., Boggess, K., Wylie,
585 B. J., Simas, T. A. M., Louis, J. M., Espinoza, J., Gaw, S. L., Murtha, A., Wiegand, S.,
586 Gollin, Y., Singh, D., Silver, R. M., Durie, D. E., Panda, B., Norwitz, E. R., ... Kilpatrick,

- 587 S. (2022). Circulating Angiogenic Factor Levels in Hypertensive Disorders of Pregnancy.
588 *NEJM Evidence*, 1(12). <https://doi.org/10.1056/EVIDOA2200161>
- 589 Wan Shumei, Peng Ping, Qiao Lin, G. Y. (2019). Expression of miR-144, titin-Ab and MAPK
590 signal transduction pathway related proteins in pre-eclampsia patients. *INTERNATIONAL*
591 *JOURNAL OF CLINICAL AND EXPERIMENTAL MEDICINE*, 11(127), 11–20.
592 www.ijcem.com /ISSN:1940-5901/IJCEM0098123
- 593 Wei, J., Fu, Y., Mao, X., Jing, Y., Guo, J., & Ye, Y. (2019). Decreased Filamin b expression
594 regulates trophoblastic cells invasion through ERK/MMP-9 pathway in pre-eclampsia.
595 *Ginekologia Polska*, 90(1), 39–45. <https://doi.org/10.5603/GP.2019.0006>
- 596 Whitehead, C. L., Walker, S. P., Ye, L., Mendis, S., Kaitu'u-Lino, T. J., Lappas, M., & Tong,
597 S. (2013). Placental specific mRNA in the maternal circulation are globally dysregulated
598 in pregnancies complicated by fetal growth restriction. *Journal of Clinical Endocrinology*
599 *and Metabolism*, 98(3). <https://doi.org/10.1210/jc.2012-2468>
- 600 Zeisler, H., Llorba, E., Chantraine, F., Vatish, M., Staff, A. C., Sennström, M., Olovsson, M.,
601 Brennecke, S. P., Stepan, H., Allegranza, D., Dilba, P., Schoedl, M., Hund, M., &
602 Verlohren, S. (2016). Predictive Value of the sFlt-1:PIGF Ratio in Women with Suspected
603 Preeclampsia. *The New England Journal of Medicine*, 374(1), 13–22.
604 <https://doi.org/10.1056/NEJMOA1414838>
- 605 Zhang, H. H., Wang, Y. P., & Chen, D. B. (2011). Analysis of nitroso-proteomes in
606 normotensive and severe preeclamptic human placentas. *Biology of Reproduction*, 84(5),
607 966–975. <https://doi.org/10.1095/BIOLREPROD.110.090688>
- 608 Zhou, A. X., Hartwig, J. H., & Akyürek, L. M. (2010). Filamins in cell signaling, transcription
609 and organ development. In *Trends in Cell Biology* (Vol. 20, Issue 2).
610 <https://doi.org/10.1016/j.tcb.2009.12.001>
- 611

612 **Supplemental Material**

613 Supplemental Methods

614 Supplemental table S1-4

615 Supplemental figure S1

616 List of differentially abundant proteins and functional enrichment analysis:

617 <https://data.mendeley.com/datasets/j2x4h9ddcj/draft?a=8ccd383c-c6e5-495d-b66b->

618 [29c691608995](https://data.mendeley.com/datasets/j2x4h9ddcj/draft?a=8ccd383c-c6e5-495d-b66b-29c691608995)

619

620

621

622

623

624

625

626

627
628
629
630
631
632
633
634
635
636
637
638
639
640
641
642
643
644
645
646
647
648

649

650

651

652

653

654

655

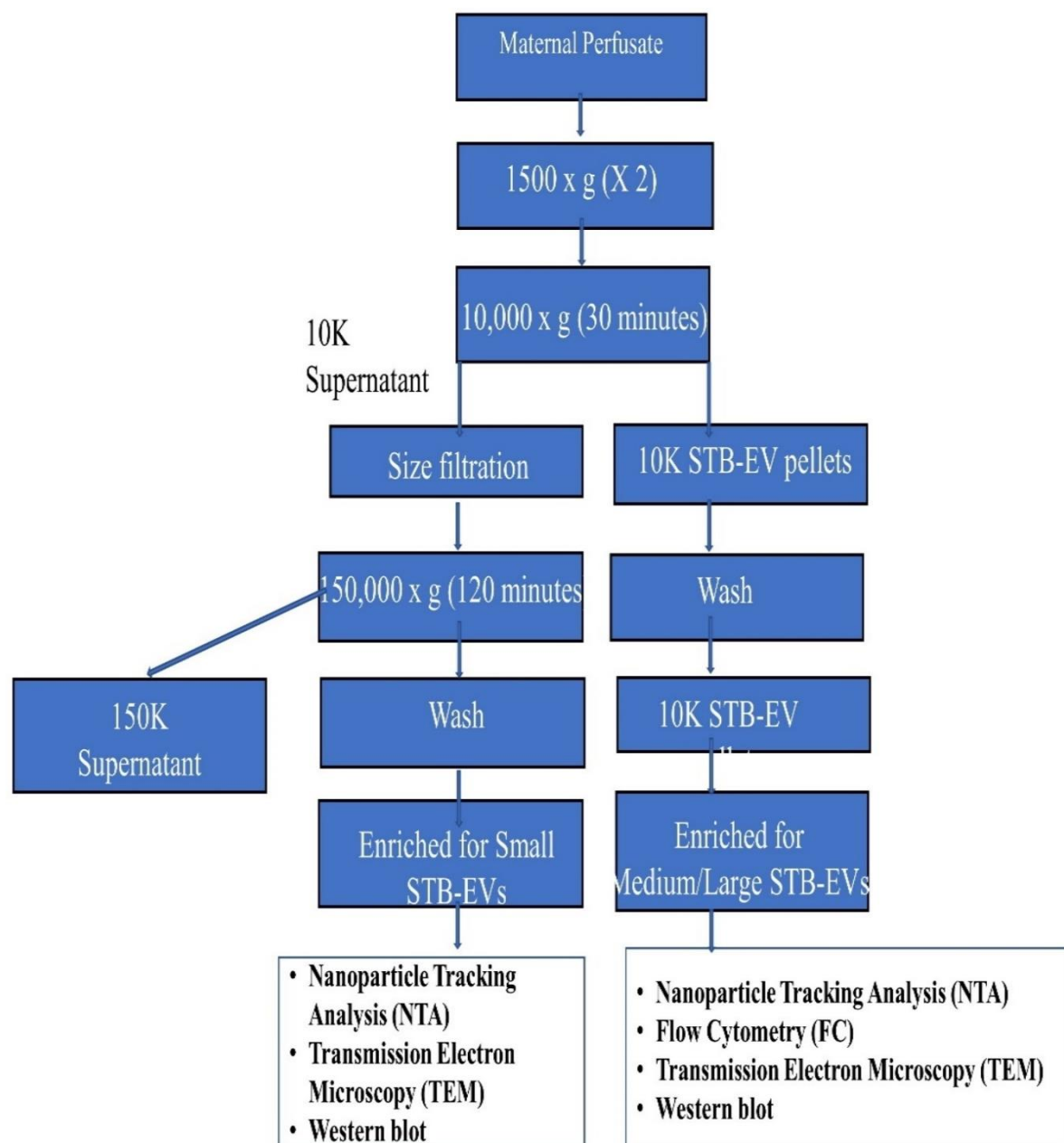
656

657

Supplemental data

658 **Supplemental methods**

659



660

661 **Supplemental figure 1.** Flow chart illustrating the steps involved in characterizing m/ISTB-

662 EVs and sSTB-EVs obtained via differential ultracentrifugation (10,000 and 150,000 g) of

663 maternal perfusate. Nanoparticle trafficking analysis, transmission electron microscopy, flow

664 cytometry, and western blot were used to characterize the pellets from both spins.

665 **Transmission electron microscopy**

666 The Sir William Dunn School of Pathology was contracted to perform transmission electron
667 microscopy. STB-EV pellets were diluted with fPBS to produce STB-EV solutions with
668 concentrations ranging from 0.1 to 0.3 g/l. For 2 minutes, ten microliter of the STB-EV pellet
669 solution was applied to freshly glowing discharged carbon formvar 300 mesh copper grids,
670 blotted with filter paper, stained with 2% uranyl acetate for 10 seconds, blotted, and air-dried.
671 The grid's STB-EV pellets are negatively stained to increase the contrast between the STB-EV
672 pellets and the background. The grids were imaged with a Gatan OneView CMOS camera on
673 an FEI Tecnai 12 TEM at 120 kV.

674 **Nanoparticle tracking analysis.**

675 The Nanosight NS500 (instrument equipped with a 405 nm laser [Malvern UK]), sCMOS
676 camera, and nanoparticle tracking analysis (NTA) software version 2.3, Build 0033 (Malvern
677 UK)) system was used for the analysis. Instrument performance was tested with silica 100
678 nm microspheres prior to sample analysis (Polysciences, Inc.). The samples were diluted in
679 fPBS to a concentration to 1/100,000 based on the starting concentration. The samples were
680 automatically injected into the sample chamber with a 1 ml syringe using the EV measurement
681 script: prime, delay of 5, capture of 60, and repeat of 4. Camera images of the analyzed samples
682 were captured at a level of 12. (Camera shutter speed; 15 ms and Camera gain; 350). NTA
683 post-acquisition settings were optimized and maintained constant across samples. Each video
684 recording was analyzed to determine the size and concentration profile of STB-EV.

685

686

687 **Western blotting**

688 **Supplemental table 1.** Reagents used for western blot.

Buffers	Power of hydrogen (pH)	Constituents
4X Laemmli reducing buffer	6.8	9 parts 4 X Laemmli buffer
		1 part 2-beta-mercaptoethanol
4X Laemmli non-reducing buffer		4 X Laemmli buffer
Anode buffer 1	10.4	300 mM Tris base (36.34 g/L)
		100 % methanol (20 mL/L)
		980 ml of ddH ₂ O
Anode buffer 2	10.4	25 mM Tris base (3.0 g/L)
		100 % methanol (20 mL/L)
		980 ml of ddH ₂ O
Cathode buffer	9.4	25 mM Tris base (3.0 g/L)
		40 nM 6-aminocaproic acid (5.2 g/L)
		100 % methanol (20 mL/L)
		980 mL of dH ₂ o
10 X TBS	8	NaCl (87.6g)
		Tris base (12.1g)
		700 ml of ddH ₂ O
TBST	8	10 X TBS (100 mL)
		0.1 % Tween-20 (1 mL)
		900 mL of ddH ₂ O
5% Milk TBST		5g of Blotto in 100 mL of TBST

689

690

691

692

693

694

695

696 **Supplemental table 2.** Antibodies used for western blot.

Antibodies	Concentration	Dilution	Antigen	Specificity	Manufacturer
Anti-PLAP (NDOG 2)	1.6 µg/µl	1/1000	PLAP	STB-EV	In house antibody
Anti-CD63	200 µg/µl	1/1000	CD63	STB-EV	Santa Cruz Biotechnology
Anti-ALIX	200 µg/µl	1/1000	ALIX	S STB-EV	Cell Signalling
Anti-Cytochrome C	200 µg/µl	1/500	Cytochrome C	Placenta homogenate	Santa Cruz Biotechnology
Anti-SR-BI	0.35 µg/µl	1/1000	SR-BI	N/A	Abcam
Anti-Filamin B	1.64 µg/µl	1/1000	Filamin B	N/A	Insight Biotechnology
Anti-PAPP-A2	1 µg/µl	1/2000	PAPP-A2	N/A	Abcam
Anti-Collagen 17 A1	1 µg/µl	1/1000	Collagen 17 A1	N/A	Abcam
Polyclonal mouse/rabbit immunoglobulin HRP	goat-anti-	1/2000	Mouse and Rabbit Immunoglobulins	N/A	Dako UK Ltd

697

698

699

700

701

702

703

704

705

706 **Bioinformatic analysis of proteomic data from placenta tissue, medium/large and small**

707 **STB-EVs**

708 Persus (Max Planck Institute of Biochemistry) was used for the analysis, along with the
709 accompanying documentation and tutorials. To remove invalid data, we pre-processed the raw
710 data by log transforming and filtering. Missing values were imputed at random from a normal
711 distribution using the following parameters: width = 0.3 and downshift = 1.8. To ensure
712 conformity to the normal distribution, the underlying distribution was visually inspected with
713 a histogram before and after missing data imputation. The data was then transformed further
714 by deducting each (transformed) value from the highest occurring protein expression value.

715 Principal component analysis (PCA), heatmaps, and Pearson correlation matrices were used to
716 further investigate the data. The data was analyzed using the correlation index and hierarchical
717 clustering. A two-sample independent student t-test was used to assess differential expression.
718 Multiple testing was corrected using permutation-based false discovery rate (FDR) with the
719 following parameters, with significance set at less than 0.05.

720

721

722

723

724

725

726

727

728

729

730 **Functional enrichment of differentially expressed proteins (DEPs) in preeclampsia (PE)**

731 **Supplemental table 3:** The top three functionally enriched gene ontologies are: biological

732 process (GO: BP) Placenta (bold font), medium/large STB-EVs (normal font), and small STB-

733 EVs (italics).

734

Biological Process (BP)	Adjusted P Values	No of Proteins in BP terms	No of DEP queried	No of DEP found in BP terms
Negative regulation of neurotransmitter secretion	0.02	2	14	2
Negative regulation of synaptic vesicle exocytosis	0.02	2	14	2
Negative regulation of neurotransmitter transport	0.05	3	14	2
Response to decreased oxygen levels	0.00	84	293	30
Cellular response to decreased oxygen levels	0.00	59	293	24
Cellular ketone metabolic process	0.00	65	293	26
<i>Peptidyl-asparagine modification</i>	<i>0.02</i>	<i>10</i>	<i>73</i>	<i>5</i>
<i>Protein N-linked glycosylation via asparagine</i>	<i>0.02</i>	<i>10</i>	<i>73</i>	<i>5</i>
<i>Protein N-linked glycosylation</i>	<i>0.02</i>	<i>16</i>	<i>73</i>	<i>6</i>

735

736

737

738

739

740

741

742

743 **Supplemental table 4:** The top three functionally enriched KEGG Pathways in the placenta,
744 medium/large STB-EVs, and small STB-EVs (only 1 KEGG). Placenta (bold font),
745 medium/large STB-EVs (normal font), and small STB-EVs (italics)

KEGG Pathways (KP)	Adjusted P Values	No of Proteins in KP terms	No of DEP queried	No of DEP found in KP terms
Neurotrophin signalling pathway	0.00	13	14	3
Long-term potentiation	0.01	6	14	2
Renal cell carcinoma	0.02	11	14	2
Proteasome	0.00	35	293	17
Spinocerebellar ataxia	0.00	48	293	21
Alzheimer disease	0.01	94	293	29
<i>Protein processing in endoplasmic reticulum</i>	<i>0.02</i>	<i>60</i>	<i>73</i>	<i>10</i>

746
747

748

749
750

751

752

753

754

755

756

757

758

759

760

761 **Major Resources Table**

762 **Antibodies**

Target antigen	Vendor or Source	Catalog #	Working concentration	Dilution
PLAP	In house antibody		1.6 µg/µl	1/1000
CD63	Santa Cruz Biotechnology	sc-365604	200 µg/µl	1/1000
ALIX	Cell Signalling	#2171	200 µg/µl	1/1000
Cytochrome C	Santa Cruz Biotechnology	sc-13560	200 µg/µl	1/500
SR-BI	Santa Cruz Biotechnology	ab52629	0.35 µg/µl	1/1000
Filamin B	Insight Biotechnology	GTX387	1.64 µg/µl	1/1000
PAPP-A2	Abcam	ab59100	1 µg/µl	1/1000
Collagen 17A1	Abcam	Ab28440	1 µg/µl	1/2000
Mouse Immunoglobulins	Dako UK Ltd	P044701	1 µg/µl	1/2000
Rabbit Immunoglobulins	Dako UK Ltd	P044801	1 µg/µl	1/2000

763
764
765
766
767
768
769
770
771
772
773
774
775
776
777
778
779
780
781
782
783
784
785
786
787
788 **Flow cytometry resources**

Markers	Fluorochromes	Clone	CAT	Isotype	Dilution / Concentration
CD41	PE Vio770	REA386	130-105-562	REA	1 in 50 for dump channel analysis.
CD235	PE Vio770	RAE-175	130-100-258	REA	
HLA Class-I (ABC)	PE Vio770	REA230	130-101-460	REA	
HLA Class-II (DRDPDQ)	PE Vio770	RAE-332	130-104-828	REA	
REA control				REA	
CD41	Pacific blue	HIP8	303713	Mouse IgG1	1 in 100
CD235	Pacific blue	HI264	349107	Mouse IgG2a	1 in 100
HLA Class-I (ABC)	Pacific blue	W6/32	311417	Mouse IgG2a	1 in 100
PLAP	PE	Mouse mAb	N/A	IgG1	0.2mg/ml
IgG2a isotype control	Pacific blue	MOPC-173	981904	IgG2a	1 in 500

IgG1 isotype control	Pacific blue	MOPC-21	400131	IgG1	1 in 200
bioM	FITC	NA	NA	NA	0.5-1nM

789

790

791

792

793

794

795